Composite-Light-Pulse Technique for High-Precision Atom Interferometry

P. Berg,[1] S. Abend,[1] G. Tackmann,[1] C. Schubert,[1] E. Giese,[2] W. P. Schleich,[2,3] F. A. Narducci,[4] W. Ertmer,[1] and E. M. Rasel[1*]

[1]*Institut für Quantenoptik and Centre for Quantum Engineering and Space-Time Research (QUEST), Leibniz Universität Hannover, Welfengarten 1, D-30167 Hannover, Germany*

[2]*Institut für Quantenphysik and Center for Integrated Quantum Science and Technology (IQ^{ST}), Universität Ulm, Albert-Einstein-Allee 11, D-89081 Ulm, Germany*

[3]*Texas A&M University Institute for Advanced Study (TIAS), Institute for Quantum Science and Engineering (IQSE), and Department of Physics and Astronomy, Texas A&M University, College Station, Texas 77843-4242, USA*

[4]*Naval Air Systems Command, EO Sensors Division, Patuxent River, Maryland 20670, USA*

(Received 31 October 2014; published 9 February 2015)

We realize beam splitters and mirrors for atom waves by employing a sequence of light pulses rather than individual ones. In this way we can tailor atom interferometers with improved sensitivity and accuracy. We demonstrate our method of composite pulses by creating a symmetric matter-wave interferometer which combines the advantages of conventional Bragg- and Raman-type concepts. This feature leads to an interferometer with a high immunity to technical noise allowing us to devise a large-area Sagnac gyroscope yielding a phase shift of 6.5 rad due to the Earth's rotation. With this device we achieve a rotation rate precision of 120 nrad s^{-1} $Hz^{-1/2}$ and determine the Earth's rotation rate with a relative uncertainty of 1.2%.

DOI: 10.1103/PhysRevLett.114.063002 PACS numbers: 37.25.+k, 03.75.Dg, 04.80.Cc, 06.30.Gv

During the last decade atom interferometry, either with cold atoms or Bose-Einstein condensates, has developed into an extremely active field, with a wealth of applications ranging from the use of gravimeters [1–3], gyroscopes [4–6], and magnetometers [7] to the determination of the photon recoil [8] and tests of the foundations of general relativity [9,10]. Improving the performance of atom interferometers relies on a maximization of the scale factor and the intrinsic suppression of technical noise. In the present Letter we introduce the method of composite light pulses to create beam splitters and mirrors which allow us to achieve both of these goals. We demonstrate our technique by realizing a symmetrized large-area Sagnac interferometer and measure the Earth's rotation rate.

Composite laser pulses, reminiscent of NMR techniques [11], have already been employed for beam splitters introducing a large momentum shift [12–15], but without taking advantage of their flexibility to suppress technical noise. Although our symmetric interferometer shows features that are similar to those based on double diffraction [16–18], the composite-light-pulse technique bears several decisive advantages: (i) Since our beam splitters are composed of conventional Raman pulses, it is straightforward to implement and easily applicable to other interferometers such as gravimeters; (ii) moreover, it allows us to scan the fringe pattern via the laser phase while still largely suppressing the influence of laser phase noise and magnetic field fluctuations.

As a consequence, our interferometer displays a rotation rate sensitivity of 120 nrad s^{-1} $Hz^{-1/2}$ being the lowest rotation noise measured by cold-atom gyroscopes [5] and reaches a resolution of 26 nrad s^{-1} at 100 s. Thanks to the reduced systematic uncertainties, we determined the Earth's rotation rate with an uncertainty of 1.2%.

Single light pulses driving narrow two-photon transitions have become a versatile tool for atom interferometers to realize beam splitters or mirrors [19]. Indeed, by tuning the pulse duration τ and the Rabi frequency such that the Rabi angle is $\pi/2$ or π, we obtain a beam splitter or a mirror, respectively. In order to achieve a high contrast with the conventional Mach-Zehnder interferometer (MZI) shown in Fig. 1(a), atoms both with a narrow velocity distribution and in a specific electronic state with only higher order magnetic susceptibility are prepared as a first step [20]. They are then coherently split, redirected, and recombined due to their interaction with three Raman pulses separated by a time T, often referred to as the $\pi/2 - \pi - \pi/2$ sequence.

Our symmetrized composite-pulse interferometer (SCI) displayed in Fig. 1(b) differs in two ways from the MZI: (i) It does not require a preparation step prior to the interferometer sequence and (ii) the beam splitter and the mirror are composed of a rapid succession of several Raman pulses separated by a minimal dark time t_S of only a few microseconds.

The first $\pi/2$ pulse of the MZI is replaced in the SCI by a $\pi/2$ pulse and a subsequent π pulse. By shifting the frequency difference of the Raman laser to match the Doppler shifted resonance, the later pulse is only resonant with the branch of the interferometer where the atoms have remained in the initial electronic state [24]. The momentum transferred in this process, by design, is inverted with respect to the one obtained by the previous $\pi/2$ pulse. In this way, the matter waves move apart from each other with twice the effective photon recoil of the MZI. After the first

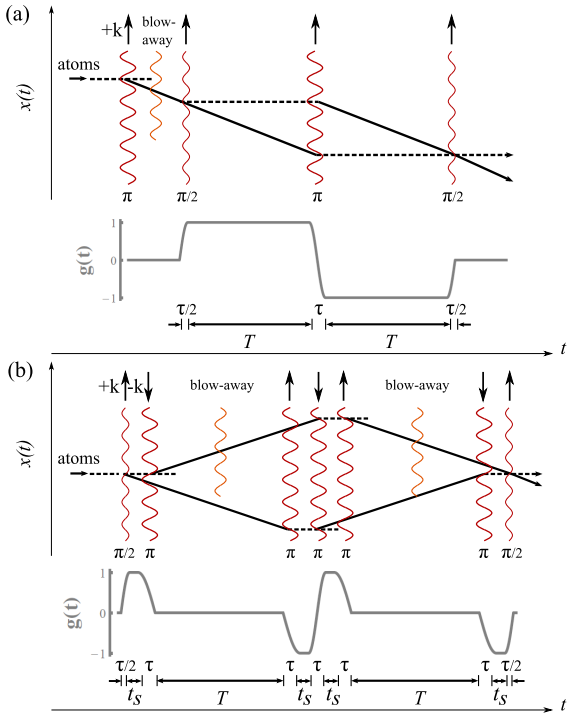

FIG. 1 (color online). Space-time diagram (x, t) and the corresponding sensitivity function $g(t)$ defined in Refs. [21,22] for (a) a conventional Mach-Zehnder interferometer (MZI) with single Raman pulses (red wavy lines) as atom-optical elements [23] and (b) the symmetrized composite-pulse interferometer (SCI) featuring multiple Raman pulses (multiple red wavy lines) for each atom-optical beam splitter and mirror. The single-pulse duration τ as well as the dark time t_S within a composite pulse is not drawn to scale. The Raman interactions lead to a change of both the electronic state (ground and excited state denoted by solid and dashed lines, respectively) and the kinetic momentum of the wave packet, depending on the direction of the effective photon momentum $\mathbf{k}$ (indicated by black arrows). The contrast of the MZI signal depends crucially on the state preparation. A pure sample of excited-state atoms can be achieved by optical pumping after molasses cooling. As shown in the figure, a specific velocity class of this sample can be selected with the help of a Raman pulse transferring them into the ground state, while the rest of the excited atoms are removed by a resonant blow-away pulse (yellow wavy lines). In contrast, in the SCI the blow-away pulse is not performed until the first two beam-splitter pulses. As indicated by $g(t)$, which expresses the sensitivity to Raman laser phase noise and magnetic field fluctuations, the SCI is insensitive to these noise sources during the free evolution time T, while the MZI is most sensitive during the same period.

beam splitter sequence a blow-away pulse removes all atoms in the initial electronic state.

In a very similar procedure, the π pulse of the MZI is extended in the SCI by two additional π pulses such that the interferometer branches are redirected towards each other. Again, a purification of the electronic state follows in this sequence.

The SCI is closed by a third sequence composed again of a π pulse and a $\pi/2$ pulse. The readout of the interference signal is accomplished by a state-selective fluorescence detection in complete analogy to the MZI.

In the MZI the Sagnac phase shift caused by a rotation rate Ω reads [25,26]

$$\Phi_{\mathrm{rot}}^{\mathrm{MZI}} \approx 2(\mathbf{k}\times\mathbf{v})\cdot\Omega T^2\left[1+\left(1+\frac{2}{\pi}\right)\frac{\tau}{T}+\cdots\right], \quad (1a)$$

where we have accounted for a nonvanishing pulse duration $\tau \ll T$ and assumed for all light pulses the same Rabi frequency. Here $\mathbf{k}$ and $\mathbf{v}$ denote the effective wave vector associated with the momentum transfer and the initial atomic velocity, respectively.

In contrast, the corresponding phase shift in the SCI is given by [27]

$$\Phi_{\mathrm{rot}}^{\mathrm{SCI}} \approx 4(\mathbf{k}\times\mathbf{v})\cdot\Omega T^2\left[1+\left(4+\frac{3}{\pi}\right)\frac{\tau}{T}+3\frac{t_S}{T}+\cdots\right], \quad (1b)$$

where $t_S \ll T^2/\tau$ is the dark time during the composite pulse. We emphasize that the scale factor of the SCI is twice the one of the MZI. Moreover, apart from the correction due to the dark time, the additional terms resulting from finite pulse durations are similar in both interferometers.

A key result of our work is that the immunity of the SCI to noninertial perturbations stems from the fact that most of the time—namely, during the time T of free evolution—the matter waves are in the same electronic state while propagating along the two branches. Therefore, the fluctuations of both the phase of the laser which drives the transition between these states and the external forces which, in general, act differently on the two internal states only affect the interferometer signal during the comparably small time intervals τ and t_S and are therefore strongly reduced as compared to the MZI.

The suppression of these noise effects is best quantified in terms of the temporal sensitivity function $g(t)$, well established in the characterization of atomic frequency standards and interferometers [21,22,28] and shown in Fig. 1 as a grey curve for each geometry. It describes the change in the signal of the interferometer due to a small phase step occurring at a specific instance t of the interferometer cycle. If only one branch of the interferometer is addressed by a light pulse, the sensitivity function will oscillate at half the Rabi frequency between -1 or 1 and 0 and it remains constant while the light is off. If both branches are manipulated, $g(t)$ will oscillate at the Rabi frequency between -1 and 1 during a light pulse.

For the SCI the sensitivity function vanishes during the free evolution time T, while in the MZI it assumes the maximum absolute value of $|g(t)| = 1$ during the same time span. Depending on the durations t_S and τ, only a small Fourier frequency band of phase fluctuations couples into the signal of the SCI.

We have implemented the SCI in a slightly modified setup of our cold-atom gyroscope [23,29], formerly

operated as a dual MZI with two counterpropagating pulsed beams of laser-cooled ^{87}Rb with a forward speed of $v = 2.79$ m/s and a repetition rate of 2 Hz. The gyroscope is mounted on a passive vibration isolation platform combining two MinusK 650BM-1 stages and shielded against acoustic noise by an enclosure. The Zeeman degeneracy of the atoms being in a hyperfine ground state is lifted by a magnetic offset field of 750 mG. Coherent manipulation with Raman pulses is performed on the hyperfine transition with zero linear magnetic susceptibility in three spatially separated zones employing retro reflectors of type Thorlabs-BB2-E03 for the light fields which are mounted on remotely controllable mirror mounts in order to align the reflectors by the interferometer itself. During these processes the laser phase is imprinted onto the atoms. Between the beam-splitter zones the atoms travel freely, allowing pulse spacings of $T_{\mathrm{MZI}} = 23$ ms and $T_{\mathrm{SCI}} = 25$ ms in the MZI and the SCI, respectively. The composite pulses are made of $\tau = 30\ \mu$s—long Raman pulses separated by $t_S = 4\ \mu$s. With these parameters, the SCI features an area of 41 mm^2, the largest demonstrated so far for a cold-atom gyroscope.

We demonstrate the coherence of the beams in the MZI and the SCI by recording the atomic population in one of the output ports in its dependence on the laser phase Φ_L (Fig. 2). The latter is stepwise increased in successive measurements by altering the phase of the last Raman laser pulse with respect to the others. From the resulting interference fringes, we deduce contrasts of 36% and 19% for the MZI and the SCI, respectively. These low values are a consequence of (i) spontaneous emission during the Raman pulses before the blow-away pulse and (ii) inhomogeneities of the Rabi frequency across the atomic cloud. These effects are even more prominent in the case of the SCI due to the higher number of atom-light interactions.

The interference pattern of Fig. 2 allows us to determine the rotational phase for both geometries. In order to distinguish it from the other phase contributions, we read out the signals of two counterpropagating interferometers with horizontal velocities $+v$ and $-v$. In our configuration one interferometer is resonant with the wave vector $+\mathbf{k}$, while the other interacts with the oppositely directed wave vector $-\mathbf{k}$. According to Eq. (1), the rotational phase remains invariant under the transformation $v \to -v$ and $\mathbf{k} \to -\mathbf{k}$ and we arrive at the total phases

$$\Phi^{\mathrm{MZI}}_{\pm v} \equiv \Phi^{\mathrm{MZI}}_{\mathrm{rot}} \pm \Phi_{\mathrm{acc}} \pm \Phi^{(\pm)}_B + \Phi^{(T+\tau)}_L$$

and

$$\Phi^{\mathrm{SCI}}_{\pm v} \equiv \Phi^{\mathrm{SCI}}_{\mathrm{rot}} \pm 2\Phi_{\mathrm{acc}} \pm \xi\Phi^{(\pm)}_B + \Phi^{(\tau_{\mathrm{cp}})}_L$$

of the two interferometers denoted by the subscripts $\pm v$ operated as a MZI and a SCI, respectively.

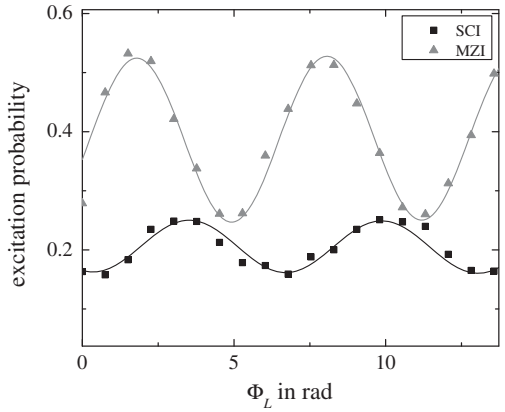

FIG. 2. Interference signals of the MZI (triangles) and the SCI (squares) obtained by scanning the phase Φ_L of the last Raman pulse. Because of an imperfect efficiency of the Raman processes, the larger number of beam-splitter pulses required in the SCI leads to a reduced contrast of 19% in the SCI as compared to the MZI, where it is 36%. From these fringes we also determine the total phase offset which contains the corresponding rotational phase shifts $\Phi^{\mathrm{MZI}}_{\mathrm{rot}}$ and $\Phi^{\mathrm{SCI}}_{\mathrm{rot}}$.

Apart from Φ_L, $\Phi^{\mathrm{MZI}}_{\mathrm{rot}}$, and $\Phi^{\mathrm{SCI}}_{\mathrm{rot}}$, the other leading phase components consisting of the linear acceleration shift $\Phi_{\mathrm{acc}} \sim \mathbf{k}$ and the magnetic field gradient shift $\Phi_B \sim v$ flip their signs for the respective counterpropagating interferometer. The superscripts $\pm$ of the magnetic phase emphasize the fact that it crucially depends on the trajectory of the atom in the two interferometers. The gradient relevant in our experiment is pointing along the atomic beams as the separation of the wave packets is still small with respect to the transverse gradient. The suppression factor $\xi \approx (2t_S + 6\tau/\pi)/T$ in front of $\Phi^{(\pm)}_B$ in the SCI mainly arises from the ratio of the time slots in which the interferometers are sensitive to these effects. Moreover, we have introduced the superscripts $T + \tau$ and τ_{cp} to stress the influence of the laser phase during these periods as expressed by the sensitivity functions in Fig. 1. Here, τ_{cp} denotes the duration of a composite pulse.

In order to extract the rotational phase, we combine the phases of the counterpropagating interferometers in the sums

$$\Phi^{\mathrm{MZI}}_{+} \equiv \Phi^{\mathrm{MZI}}_{+v} + \Phi^{\mathrm{MZI}}_{-v} = 2\Phi^{\mathrm{MZI}}_{\mathrm{rot}} + \Delta\Phi_B + 2\Phi^{(T+\tau)}_L$$

and

$$\Phi^{\mathrm{SCI}}_{+} \equiv \Phi^{\mathrm{SCI}}_{+v} + \Phi^{\mathrm{SCI}}_{-v} = 2\Phi^{\mathrm{SCI}}_{\mathrm{rot}} + \xi\Delta\Phi_B + 2\Phi^{(\tau_{\mathrm{cp}})}_L.$$

We emphasize that the difference $\Delta\Phi_B \equiv \Phi^{(+)}_B - \Phi^{(-)}_B$ vanishes only if the trajectories of the two counterpropagating interferometers overlap perfectly, while this does not hold for temporal fluctuations. Hence, in general, there is a residual magnetic contribution in the MZI which in the SCI is intrinsically suppressed by the factor ξ.

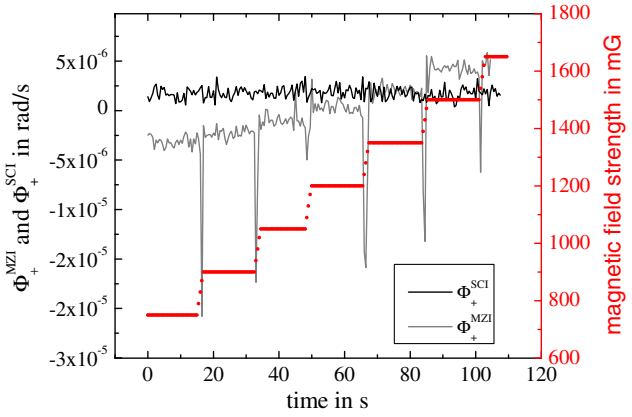

FIG. 3 (color online). Time series of the sum phases Φ_+^{MZI} (grey) and Φ_+^{SCI} (black) expressed in units of a relative rotation rate for a stepwise increasing magnetic offset field (red). The changes in the MZI rotation signal are caused by transients occurring when the magnetic field is changed while the interferometer operates. In contrast, the SCI signal given by the horizontal line is unaffected by these perturbations.

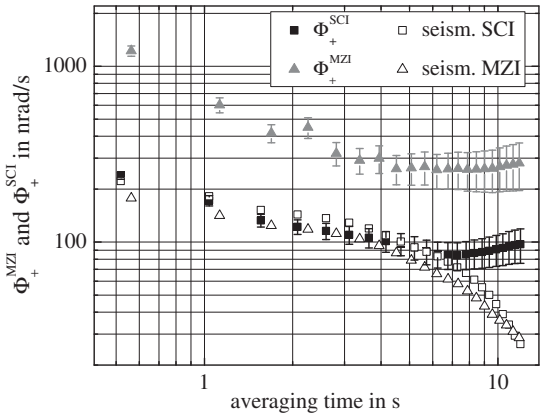

FIG. 4. Two-sample standard deviations of the interferometer sum phases Φ_+^{MZI} (full triangles) and Φ_+^{SCI} (full squares). Whereas Φ_+^{MZI} is strongly affected by the phase noise of the Raman laser, Φ_+^{SCI} is hardly influenced by it. During the measurements we monitor the rotational noise by the differential signal of two seismometers (empty symbols) positioned at the ends of the platform.

We have verified this remarkable feature of the SCI by increasing the magnetic offset field in discrete steps of about 150 mG while operating the interferometers. The resulting time series of Φ_+^{MZI} and Φ_+^{SCI} are depicted in Fig. 3, where, for comparison, the phases were scaled in units of a relative rotation rate.

The phase Φ_+^{MZI} follows the steps in the magnetic field strength and exhibits huge dips due to transients introduced by the stepwise increase during the interferometer sequence. In contrast, no significant perturbations occur in Φ_+^{SCI}. By the same mechanism the SCI suppresses the influence of fluctuations of the magnetic field, which allows us to directly determine the rotational phase $\Phi_{\mathrm{rot}}^{\mathrm{SCI}}$ by deliberately setting $\Phi_L = 0$.

Although the dc component of Φ_L is reliably controllable, the sensitivity to rotations can be harmed by its ac components. Their suppression in $\Phi_L^{(\tau_{\mathrm{cp}})}$ as compared to $\Phi_L^{(T+\tau)}$ is confirmed by the comparison of the noise in Φ_+^{MZI} and Φ_+^{SCI}, depicted as a two-sample standard deviation in Fig. 4.

For this measurement we have used a standard rf synthesizer as a phase reference for the Raman pulses. The stability of the MZI is strongly affected by the synthesizer phase noise at 700 nrad s^{-1} $\mathrm{Hz}^{-1/2}$, as confirmed by the use of a low-noise microwave reference, whereas the SCI suppresses the noise by 11 dB. In the latter case the noise is due mainly to rotations of the platform, as verified by correlating the signal with two seismometers.

The best performance of the SCI gyroscope with a precision of 120 nrad s^{-1} $\mathrm{Hz}^{-1/2}$ was obtained during a quiet period on the weekend, employing a high performance microwave reference for the Raman laser. This value represents an improvement compared to the instability achieved in Ref. [5] and is close to the intrinsic noise level of the device given by 77 nrad s^{-1} $\mathrm{Hz}^{-1/2}$, which is slightly below the performance reported in Ref. [4]. An even lower value of 0.6 nrad s^{-1} $\mathrm{Hz}^{-1/2}$ was obtained for a narrower detection bandwidth with a thermal beam interferometer [6]. This device strongly benefits from its continuous measurement scheme as well as a higher atomic flux but features a baseline that exceeds the one of our cold-atom gyroscope by an order of magnitude.

We have measured the Earth's rotation rate with an inaccuracy of about 600 nrad s^{-1}, corresponding to 1.2%. The uncertainty is more than one order of magnitude larger than the resolution of 26 nrad s^{-1} obtained with our setup by integrating the signal over 100 s. This measurement was performed with a slightly higher short-term instability of 260 nrad s^{-1} $\mathrm{Hz}^{-1/2}$ as we removed the acoustic shielding which caused thermal drifts of the retroreflectors of the interferometer [30]. The long-term instability of our gyroscope is a factor of 2.6 higher than the one in Ref. [5], which was integrating over 1000 s. Before now, the lowest long-term instability was obtained in Ref. [6] by integrating over 2000 s.

The inaccuracy of our measurement is dominated by the systematic uncertainties in the launch velocity of the atoms as well as their starting position combined with the relative wave front alignment of the Raman light beams. These errors can be inferred from the Sagnac formula, Eq. (1), which depends on the cross product of the effective wave vector and the atomic velocity. In order to improve on the accuracy and precision obtainable with molasses cooling, a combination of ultracold atoms with Bloch oscillations can be employed for the atom launch [31].

In conclusion, we have employed composite light pulses to realize an atom interferometer which surpasses current cold-atom gyroscopes in both area and sensitivity to rotations. Because of its flexibility, our composite-light-pulse technique

can also be employed in other applications, such as gravimetry, or in tests of the foundations of physics. The interferometer is fundamentally immune to internal-state dependent forces because the atoms traveling through the interferometer most of the time remain in the same electronic state, in contrast to the standard MZI. Moreover, the immunity to noise will be extremely beneficial for very long baseline atom interferometers, where large magnetic shields and low-noise lasers for coherent manipulation of the atoms are required [32–34]. Finally, we envision extensions to Bragg pulses and Bose-Einstein condensates.

We thank P. Bouyer for providing us with two Minus-K vibration isolation platforms, which were crucial for obtaining our results. This work was supported in part by the Deutsche Forschungsgemeinschaft (Grant No. SFB407), the European Union [Contract No. 012986-2, New and Emerging Science and Technologies (NEST), Future Inertial Atomic Quantum Sensors (FINAQS), Euroquasar, Inertial Atomic and Photonic Quantum Sensors (IQS)], and the Centre for Quantum Engineering and Space-Time Research (QUEST). G. T. acknowledges the support by the Max-Planck-Gesellschaft, the International Cold Atom Network (INTERCAN), and the Université franco-allemande, Deutsch-Französische Hochschule (UFA-DFH). E. G. is grateful to the Center for Integrated Quantum Science and Technology (IQ^{ST}) for a fellowship. W. P.S. is thankful to Texas A&M University for a Texas A&M University Institute for Advanced Study (TIAS) Faculty Fellowship and F. A .N. acknowledges funding from a Nanoscale Informal Science Education (NISE) Technology Transition grant.

*rasel@iqo.uni-hannover.de

[1] Z.-K. Hu, B.-L. Sun, X.-C. Duan, M.-K. Zhou, L.-L. Chen, S. Zhan, Q.-Z. Zhang, and J. Luo, Phys. Rev. A **88**, 043610 (2013).
[2] A. Louchet-Chauvet, T. Farah, Q. Bodart, A. Clairon, A. Landragin, S. Merlet, and F. Pereira Dos Santos, New J. Phys. **13**, 065025 (2011).
[3] A. Peters, K. Y. Chung, and S. Chu, Nature (London) **400**, 849 (1999).
[4] J. K. Stockton, K. Takase, and M. A. Kasevich, Phys. Rev. Lett. **107**, 133001 (2011).
[5] A. Gauguet, B. Canuel, T. Lévèque, W. Chaibi, and A. Landragin, Phys. Rev. A **80**, 063604 (2009).
[6] D. S. Durfee, Y. K. Shaham, and M. A. Kasevich, Phys. Rev. Lett. **97**, 240801 (2006).
[7] J. P. Davis and F. A. Narducci, J. Mod. Opt. **55**, 3173 (2008).
[8] R. Bouchendira, P. Cladé, S. Guellati-Khélifa, F. Nez, and F. Biraben, Phys. Rev. Lett. **106**, 080801 (2011).
[9] H. Müntinga *et al.*, Phys. Rev. Lett. **110**, 093602 (2013).
[10] D. Schlippert, J. Hartwig, H. Albers, L. L. Richardson, C. Schubert, A. Roura, W. P. Schleich, W. Ertmer, and E. M. Rasel, Phys. Rev. Lett. **112**, 203002 (2014).
[11] D. A. Braje, S. A. DeSavage, C. L. Adler, J. P. Davis, and F. A. Narducci, J. Mod. Opt. **61**, 61 (2014).
[12] S.-w. Chiow, T. Kovachy, H.-C. Chien, and M. A. Kasevich, Phys. Rev. Lett. **107**, 130403 (2011).
[13] J. E. Debs, P. A. Altin, T. H. Barter, D. Döring, G. R. Dennis, G. McDonald, R. P. Anderson, J. D. Close, and N. P. Robins, Phys. Rev. A **84**, 033610 (2011).
[14] H. Müller, S.-w. Chiow, S. Herrmann, and S. Chu, Phys. Rev. Lett. **102**, 240403 (2009).
[15] J. M. McGuirk, M. J. Snadden, and M. A. Kasevich, Phys. Rev. Lett. **85**, 4498 (2000).
[16] E. Giese, A. Roura, G. Tackmann, E. M. Rasel, and W. P. Schleich, Phys. Rev. A **88**, 053608 (2013).
[17] N. Malossi, Q. Bodart, S. Merlet, T. Lévèque, A. Landragin, and F. Pereira Dos Santos, Phys. Rev. A **81**, 013617 (2010).
[18] T. Lévèque, A. Gauguet, F. Michaud, F. Pereira Dos Santos, and A. Landragin, Phys. Rev. Lett. **103**, 080405 (2009).
[19] M. Kasevich and S. Chu, Phys. Rev. Lett. **67**, 181 (1991).
[20] M. Kasevich, D. S. Weiss, E. Riis, K. Moler, S. Kasapi, and S. Chu, Phys. Rev. Lett. **66**, 2297 (1991).
[21] G. J. Dick, J. D. Prestage, C. A. Greenhall, and L. Maleki, in *Proceedings of the 22nd Annual Precise Time and Time Interval (PTTI) Applications and Planning Meetings, Vienna, VA, 1990* (NASA, Washington, DC, 1991).
[22] G. Santarelli, C. Audoin, A. Makdissi, P. Laurent, G. J. Dick, and C. Clairon, IEEE Trans. Ultrason. Ferroelectr. Freq. Control **45**, 887 (1998).
[23] G. Tackmann, P. Berg, C. Schubert, S. Abend, M. Gilowski, W. Ertmer, and E. M. Rasel, New J. Phys. **14**, 015002 (2012).
[24] At the same time, the atoms in the off-resonant branch are performing a detuned Rabi oscillation and couple to a higher momentum state. The atoms during this process transferred into the initial electronic state are removed by the blow-away pulse. However, the atoms remaining in the off-resonant branch experience an additional phase shift. Whereas this phase cancels out in a perfectly symmetric interferometer, an intensity imbalance between the first and the third light pulse of 5% leads to an additional phase shift of 20 mrad in the single interferometer, which is below the uncertainty of our measurement caused by other effects.
[25] C. Antoine, Phys. Rev. A **76**, 033609 (2007).
[26] R. Stoner, D. Butts, J. Kinast, and B. Timmons, J. Opt. Soc. Am. B **28**, 2418 (2011).
[27] P. Berg, Ph.D. thesis, Leibniz Universität Hannover, 2014.
[28] P. Cheinet, B. Canuel, F. Pereira Dos Santos, A. Gauguet, F. Yver-Leduc, and A. Landragin, IEEE Trans. Instrum. Meas. **57**, 1141 (2008).
[29] T. Müller, M. Gilowski, M. Zaiser, P. Berg, C. Schubert, T. Wendrich, W. Ertmer, and E. M. Rasel, Eur. Phys. J. D **53**, 273 (2009).
[30] G. Tackmann, P. Berg, S. Abend, C. Schubert, W. Ertmer, and E. M. Rasel, C. R. Phys. **15**, 884 (2014).
[31] S. M. Dickerson, J. M. Hogan, A. Sugarbaker, D. M. S. Johnson, and M. A. Kasevich, Phys. Rev. Lett. **111**, 083001 (2013).
[32] S. Dickerson, J. M. Hogan, D. M. S. Johnson, T. Kovachy, A. Sugarbaker, S.-w. Chiow, and M. A. Kasevich, Rev. Sci. Instrum. **83**, 065108 (2012).
[33] A. Sugarbaker, S. M. Dickerson, J. M. Hogan, D. M. S. Johnson, and M. A. Kasevich, Phys. Rev. Lett. **111**, 113002 (2013).
[34] L. Zhou, Z. Y. Xiong, W. Yang, B. Tang, W. Peng, K. Hao, R. B. Li, M. Liu, J. Wang, and M. S. Zhan, Gen. Relativ. Gravit. **43**, 1931 (2011).